Journal of Physics: Conference Series **2586** (2023) 012074 doi:10.1088/1742-6596/2586/1/012074

Dual nature of low-energy isoscalar monopole and dipole states in light nuclei

V O Nesterenko

Laboratory of Theoretical Physics, Joint Institute for Nuclear Research, Dubna, Moscow region, 141980, Russia

E-mail: nester@theor.jinr.ru

Abstract. Isoscalar monopole (IS0) and dipole (IS1) states located below and around the alpha-particle threshold S_α in prolate ^{24}Mg are investigated within fully self-consistent Skyrme Quasiparticle Random-Phase Approximation (QRPA) approach. It is shown that these states demonstrate strong mean-field (MF) effects: dipole vorticity, deformation-induced monopole-quadrupole (IS0/IS2) and dipole-octupole (IS1/IS3) coupling. At the same time, the density distributions show precursors of a cluster structure. So we get a cluster/MF duality with a strong dominance of MF impact. IS0 QRPA results are compared with iThemba Lab and RCNP (α, α') data.

1. Introduction

In light nuclei, IS0 and IS1 states located below isoscalar giant monopole resonance (IS-GMR) and isovector giant dipole resonance (IV-GDR) can be treated as possible fingerprints of a cluster structure [1, 2, 3]. At the same time, these states demonstrate clear mean-field features, for example, dipole toroidal vorticity and deformation-induced dipole-octupole (IS1/IS3) [4, 5, 6, 7] and monopole-quadrupole (IS0/IS2) [7, 8, 9, 10] couplings. This manifests a cluster/MF duality [11, 12] with a coexistence of cluster and MF properties in a large energy range, both below and above the α-particle threshold S_α. It is suggested that clustering is embedded already in the ground state of a light nucleus and just IS0 and IS1 transitions allow to activate cluster degrees of freedom [1, 2, 3].

It is natural to expect that MF features dominate at excitation energies $E < S_\alpha$ while clustering becomes important at $E \geq S_\alpha$. However the actual picture is more complicated and each 0^+ or 1^- state can demonstrate its own individual interplay of cluster and MF features, depending on the structure of the state. For solution of this problem, comparative microscopic calculations within various self-consistent models are most suitable. Below we present several remarkable examples of MF features of IS0 and IS1 states in deformed ^{24}Mg, explored within fully self-consistent Skyrme QRPA [13, 14, 15, 16, 17]. For the case of the dipole vorticity, we demonstrate that Skyrme QRPA results are well confirmed by calculations within Antisymmetrized Molecular Dynamics (AMD) method [1, 2, 3, 18] relevant for exploration of both cluster and MF degrees of freedom.

2. Individual toroidal IS1 states

As a first example, let us consider dipole toroidal vorticity in axially deformed ^{24}Mg. Skyrme QRPA calculations [4, 5, 6, 7] show that the lowest $I^\pi K = 1^-1$ state in this nucleus should be toroidal. For Skyrme force SLy6 [19], this state lies at 7.92 MeV, i.e. somewhat below the threshold S_α=9.3 MeV. Fig. 1 shows that proton and neutron currents in this state exhibit a typical toroidal flow when nucleons move like on a surface of a torus pointed along x-axis [4, 6]. This kind of a vortical flow is well known in hydrodynamics as a Hill's vortex ring [20]. Being vortical, such nuclear excitations do not contribute to the continuity equation and thus provide a new promising way for investigation of nuclear vorticity.

The similarity of proton and neutron currents in Fig. 1 confirms the IS character of this excitation. Besides, this state demonstrates a large IS toroidal strength [7]. Similar results for ^{24}Mg were obtained within the AMD model [21]. Altogether, we get a remarkable example of a low-lying individual toroidal IS1 state. Individual IS1 states were also predicted in ^{20}Ne [5], ^{10}Be and [22], ^{12}C [23] and ^{16}O [24]. This means that strong IS1 transitions in light nuclei can be caused not only by clustering but also by IS dipole vorticity.

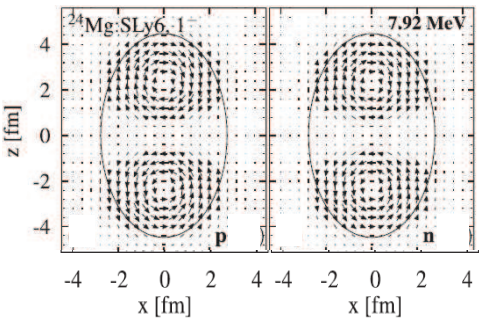

Figure 1. Proton and neutron convective currents in x-z plane for $I^\pi K = 1^-1$ 7.92-MeV state in ^{24}Mg, calculated within QRPA with Skyrme force SLy6. Solid line indicates the nuclear surface.

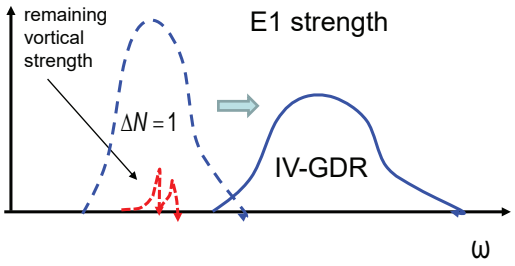

Figure 2. Schematic picture illustrating appearance of E1 vortical states in nuclei. There are $1p1h$ E1 ΔN=1 strength (dashed blue line), IV GDR strength (solid blue line) and vortical E1 strength (dashed red line). The bold arrow exhibits the action of isovector residual interaction.

The dipole toroidal vorticity (in terms of individual low-lying states [4, 5, 6, 7, 10, 21, 22, 23, 24] and toroidal dipole resonance (TDR) [25, 26, 27, 28, 29, 30, 31, 32]) is a general feature of atomic nuclei irrespective of their charge, mass number and shape. Fig. 2 illustrates the origin of the dipole vorticity. Initially, $E1$ particle-hole ($1p1h$) excitations are produced by $E1(\Delta N{=}1)$ transitions where N is the principal shell quantum number. These transitions give a strong bump denoted in the figure by the dashed blue line. The bump includes both irrotational and vortical excitations with a strong dominance of the irrotational fraction. Further, the IV dipole residual interaction upshifts most of the irrotational E1 strength and forms IV-GDR (solid blue line). Instead, the vortical E1 strength is not much affected. It remains almost at the same excitation energy (dashed red line) where it becomes already dominant. Thus, we get the TDR. Since IV strength is mainly upshifted, the remaining vortical strength becomes essentially IS.

3. Deformation-induced IS1/IS3 and IS0/IS2 couplings

In Figs. 3-4, we show next two examples of MF impact on IS1 and IS0 states. Fig. 3 exhibits IS1 and IS3 reduced transition probabilities for $K^\pi = 0^-$ and 1^- QRPA states in ^{24}Mg [7]. The IS1 strength is actually the second-order compression dipole strength, see more details elsewhere [7]. We see a clear correspondence between IS1 and IS3 responses, which is a consequence

of the deformation-induced coupling between dipole and octupole modes. Fig. 3 shows that the mentioned above $K^\pi = 1^-$ state at 7.92 MeV, though being mainly vortical/toroidal, has nevertheless a minor irrotational compression dipole component with $B(IS11)$ ~20 fm^6. Besides, this state has some IS31 admixture which results in a noticeable $B(IS31)$ strength. Since ^{24}Mg is strongly deformed, this octupole admixture can essentially affect the $B(IS11)$ value. This impact should be taken into account in addition to a possible impact of the cluster structure.

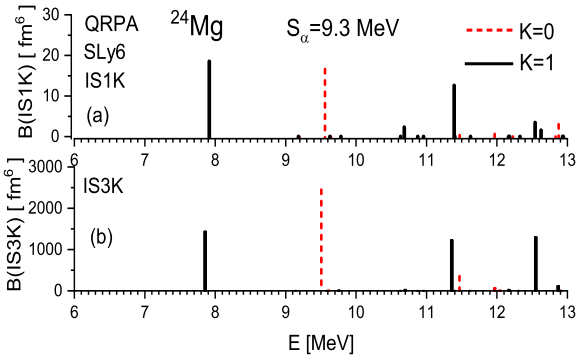

Figure 3. IS1 (a) and IS3 (b) reduced transition probabilities for $K^\pi = 0^-$ (dashed red line) and 1^- (solid black line) QRPA (SLy6) states in ^{24}Mg.

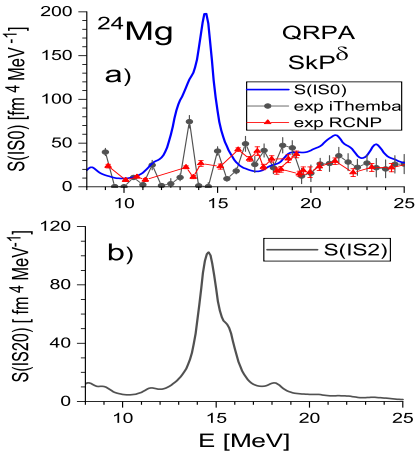

Figure 4. QRPA IS0 (a) and IS2(K=0) (b) strengths in ^{24}Mg calculated with the force SkP$^\delta$. In the upper panel, the IS0 strength function is compared with the iThemba Lab [10] and RCNP [8, 9] data.

Further, in Fig. 4 we compare IS0 monopole and IS2(K=0) quadrupole QRPA strength functions in ^{24}Mg, calculated with Skyrme force SkP$^\delta$ [33]. The strength functions use the Lorentz weight with the averaging parameter 1 MeV. It is seen that $S(IS0)$ is in good agreement with the recent iThemba Lab (α, α') data [10]. In particular, the prominent IS0 peak at 13.9 MeV is well reproduced. The comparison of QRPA IS0 an IS2 strengths shows that this peak is mainly produced by the deformation-induced IS0/IS2 coupling. The pronounced 13.9-MeV peak also takes pace in TAMU (α, α') [34] and coincidence (^{6}Li,^{6}Li$'$) [35] data but not so much in RCNP (α, α') data [8, 9] (shown in Fig. 4), see more discussion in [10]. At the same time, data [8, 9] show signatures of IS0/IS2 coupling for excitations at 16-17 MeV.

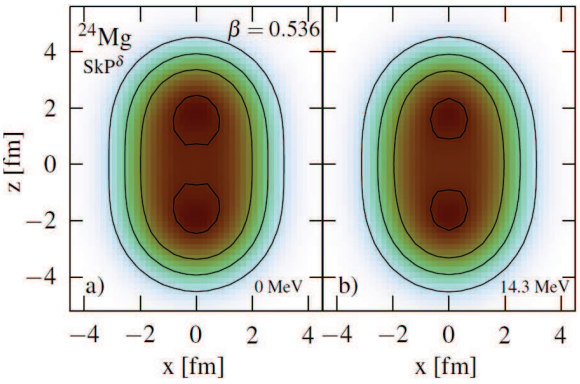

Figure 5. Nuclear density in x-z plane for the ground (a) and excited (14.3 MeV) $K^\pi = 0^+$ states in ^{24}Mg, calculated with the force SkP$^\delta$.

Finally, in Fig. 5 we show QRPA density profiles for the ground state and excited 14.3-MeV

0^+ state in ^{24}Mg [10]. The state at 14.3 MeV can be considered as a counterpart of the observed 13.9-MeV state. Both the calculated and observed states lie above the α-particle threshold S_α=9.3 MeV. Moreover, following the coincident experiment [35], the 13.8-MeV state is located close to the thresholds of ^{12}C + ^{12}C and ^{16}O + 2α cluster configurations. Fig. 5 shows that, in both the ground and excited states, there are clear cluster precursors visible as two areas of the enhanced density in the pole regions. So, our QRPA calculations do not contradict a cluster structure in deformed ^{24}Mg.

Altogether, our QRPA analysis shows that strong IS1 and IS0 transitions in light nuclei cannot be treated solely as indication of the clustering. Such transitions can be also caused by MF effects, e.g., by nuclear IS vorticity and deformation-induced IS1/IS3 and IS0/IS2 couplings. These MF effects can essentially change the strength of IS transitions. For the reliable treatment of low-lying IS states in light nuclei, we need microscopic calculations within various self-consistent models addressing both MF and cluster degrees of freedom.

Acknowledgments

VON thanks Prof. I Usman and Dr. A Bahini for provision of iThemba (α, α') data and Dr. A Repko and Profs. J Kvasil and P-G Reinhard for fruitful collaboration.

[1] Chiba Y and Kimura M 2015 *Phys. Rev.* C **91** 061302
[2] Chiba Y, Kimura M and Taniguchi Y 2016 *Phys. Rev.* C **93** 034319
[3] Chiba Y, Taniguchi Y, and Kimura M 2017 *Phys. Rev.* C **95** 044328
[4] Nesterenko V O , Repko A, Kvasil J, and Reinhard P-G, 2018 *Phys. Rev. Lett.* **120** 182501
[5] Nesterenko V O, Kvasil J, Repko A, and Reinhard P-G 2018 *Eur. Phys. J. Web of Conf.* **194** 03005
[6] Nesterenko V O, Repko A, Kvasil J, and Reinhard P-G 2019 *Phys. Rev.* C **100** 064302
[7] Adsley P et al. 2021 *Phys. Rev.* C **103** 044315
[8] Gupta Y K et al. 2015 *Phys. Lett.* B **748** 343; Erratum: 2015 *Phys. Lett.* B **751** 597
[9] Gupta Y K et al. 2016 *Phys. Rev.* C **93** 044324
[10] Bahini A et al. 2022 *Phys. Rev.* C **105** 024311
[11] Perring J K and Skyrme T H R 1956 *Proc. Phys. Soc.* **69** 600
[12] Bayman B F and Bohr A 1958 *Nucl. Phys.* **9** 596
[13] Bender M, Heenen P-H and Reinhard P-G 2003 *Rev. Mod. Phys.* **75** 121
[14] Repko A, Kvasil J, Nesterenko V O and Reinhard P-G 2015 arXiv:1510.01248[nucl-th]
[15] Repko A, Kvasil J, Nesterenko V O and Reinhard P-G 2017 *Eur. Phys. J.* A **53** 221
[16] Repko A, Kvasil J, and Nesterenko V O 2019 *Phys. Rev.* C **99** 044307
[17] Kvasil J, Repko A and Nesterenko V O 2019 *Eur. Phys. J.* A **55** 213
[18] Kanada-En'yo Y and Horiuchi H 2018 *Front. Phys.* **13** 132108
[19] Chabanat E, Bonche P, Haense P, Meyer J and Schaeffer R 1998 *Nucl. Phys.* A**635** 231
[20] Hill M J M 1894 *Phil. Trans. Roy. Soc.* A **185** 213
[21] Chiba Y, Kanada-En'yo Y and Shikata Y 2021 *Phys. Rev.* C **103** 064311
[22] Kanada-En'yo Y and Shikata Y 2017 *Phys. Rev.* C **95** 064319
[23] Kanada-En'yo Y, Shikata Y and Morita H 2018 *Phys. Rev.* C **97** 014303
[24] Kanada-En'yo Y and Shikata Y 2019 *Phys. Rev.* C **100** 014301
[25] Semenko S F 1981 *Sov. J. Nucl. Phys.* **34** 356
[26] Bastrukov S I, Mişicu Ş and Sushkov A V 1993 *Nucl. Phys.* A **562** 191
[27] Colo G, Van Giai N, Bortignon P F and Quaglia M R 2000 *Phys. Lett.* B **485** 362
[28] Vretenar D, Paar N, Ring P and Nikšić T 2002 *Phys. Rev.* C **65** 021301(R)
[29] Ryezayeva N et al. 2002 *Phys. Rev. Lett.* **89** 272502
[30] Kvasil J, Nesterenko V O, Kleinig W, Reinhard P-G and Vesely P 2011 *Phys. Rev.* C **84** 034303
[31] Repko A, Reinhard P-G, Nesterenko V O and Kvasil J 2013 *Phys. Rev.* C **87** 024305
[32] Repko A, Nesterenko V O, Kvasil J, and Reinhard P-G 2019 *Eur. Phys. J.* A **55** 242
[33] Dobaczewski J, Nazarewicz W and Werner T R 1995 *Phys. Scripta* T **56** 15
[34] Youngblood D H, Lui Y-W, Chen X F and Clark H L 2009 *Phys. Rev.* C **80** 064318
[35] Kawabata T 2013 *Few-Body Syst.* **54** 1457